Misbinding of color and motion in human early visual cortex: Evidence from event-related potentials

cortex has been suggested to be involved in the reentrant processes, as evidenced by functional magnetic resonance imaging (fMRI), transcranial magnetic stimulation (TMS), and neuropsychological studies (Colby & Goldberg, 1999; Esterman, Verstynen, & Robertson, 2007; Friedman-Hill, Robertson, & Treisman, 1995; Koivisto & Silvanto, 2012; Robertson, 2003; Shafritz, Gore, & Marois, 2002) showing that this area could modulate feature binding but had little inßuence on feature detection. Besides the binding mechanism at a relatively late stage of visual information processing, some researchers proposed that binding could also take place at an early stage of visual processing, even in the absence of attention. Their conjecture is mainly based on psychophysical Þndings on rapid feature integration (Bodel—n, Fallah, & Reynolds, 2007; Holcombe & Cavanagh, 2001) and visual contingent aftereffects (Humphrey & Goodale, 1998; Wolfe & Cave, 1999). It is known that visual contingent aftereffects are conÞned to the position of adaptation (Gibson & Radner, 1937; Stromeyer, 1972), that there is a lack of interocular transfer (Mayhew & Anstis, 1972), and that they could be induced by adaptation to locally paired dots that moved in opposite directions (Blaser, Papathomas, & Vidny‡nszky, 2005). These Þndings are taken as evidence for early binding mechanisms that are dependent on spatial and/or temporal proximity of visual features.

Although signiÞcant progress has been made in understanding the binding mechanism, we still know little about its neural implementation. Furthermore, there is a notable shortcoming of most previous studies for addressing the binding problem. In these studies, visual features were presented simultaneously and superimposed. Many neurons in almost all visual cortical areas are now known to code features in multiple dimensions. For example, many color sensitive neurons in V2 are jointly selective for other features, such as motion direction and size (Gegenfurtner, Kiper, & Fenstemaker, 1996). Therefore, the reported binding effects could be ascribed to the physical co-occurrence of features and the sensory representation of feature pairing. It is difÞcult to know whether the mechanism normally responsible for active feature binding (i.e., perceptual binding) is actually recruited (Di Lollo, 2012; Whitney, 2009).

To address the issues raised above, it is necessary to test conditions in which features are perceptually misbound and investigate how misbinding is realized in the brain, because it is likely that feature misbinding provides the strongest evidence for the existence of the active binding mechanism (Treisman & Schmidt, 1982). Wu, Kanai, and Shimojo (2004) described a vivid and compelling illusion demonstrating a steady-state misbinding of color and motion, which provided a powerful tool to investigate the neural mechanisms of feature misbinding. In a recent study (Zhang, Qiu, Zhang, Han, & Fang, 2014), we used a slightly modiÞed version of their illusion. Our stimulus (Fig. 1A, the left panel) consisted of two sheets of isoluminant dots. One sheet moved up and the other one moved down. On both sheets, dots in the right end (right of the white dashed line, the effect part) and those in the rest area (the induction part) were rendered in different colors (red or green). Oppositely moving dots always had different colors. Thus, the induction and effect parts of the stimuli combined color and motion in opposite fashions. Interestingly, when Þxating at the center of the stimuli, during most of the viewing time, observers erroneously perceived the dots in the effect part Ð the color and motion of these dots were perceptually bound in the same fashion as those in the induction part. To be more speciÞc, dots in the induction and effect parts of the upward-moving sheet were red and green, respectively. Dots in the corresponding parts of the downward-moving sheet were green and red, respectively. The color-motion misbinding made observers to perceive the effect part consisting of upward-moving red dots and downward-moving green dots.

We used psychophysical adaptation and fMRI adaptation to search for the cortical representation of the color-motion misbinding. We found that, the color-contingent motion aftereffect (CCMAE) generated from adaptation to the effect part of the illusory stimuli followed the prediction by the perceived binding (i.e., the misbinding) of color and motion rather than by the physical binding. The color-contingent motion adaptation effect in V2 measured by fMRI was found to be strongly associated with the CCMAE. Furthermore, effective connectivity analyses using dynamic causal modeling (DCM) showed that the enhanced feedback from V4 and V5 to V2 might contribute to the misbinding (Zhang et al., 2014). These Þndings strongly support the view that the binding mechanism can be implemented in early visual cortex, which is enabled by cortical feedback from higher cortical areas.

In this study, we used similar stimuli and adaptation paradigm, but with another brain imaging technique Ð event-related potential (ERP), to probe the neural mechanisms of the color-motion misbinding. We asked subjects to adapt to the color-motion misbinding, and then measured the ERPs responding to test stimuli that moved

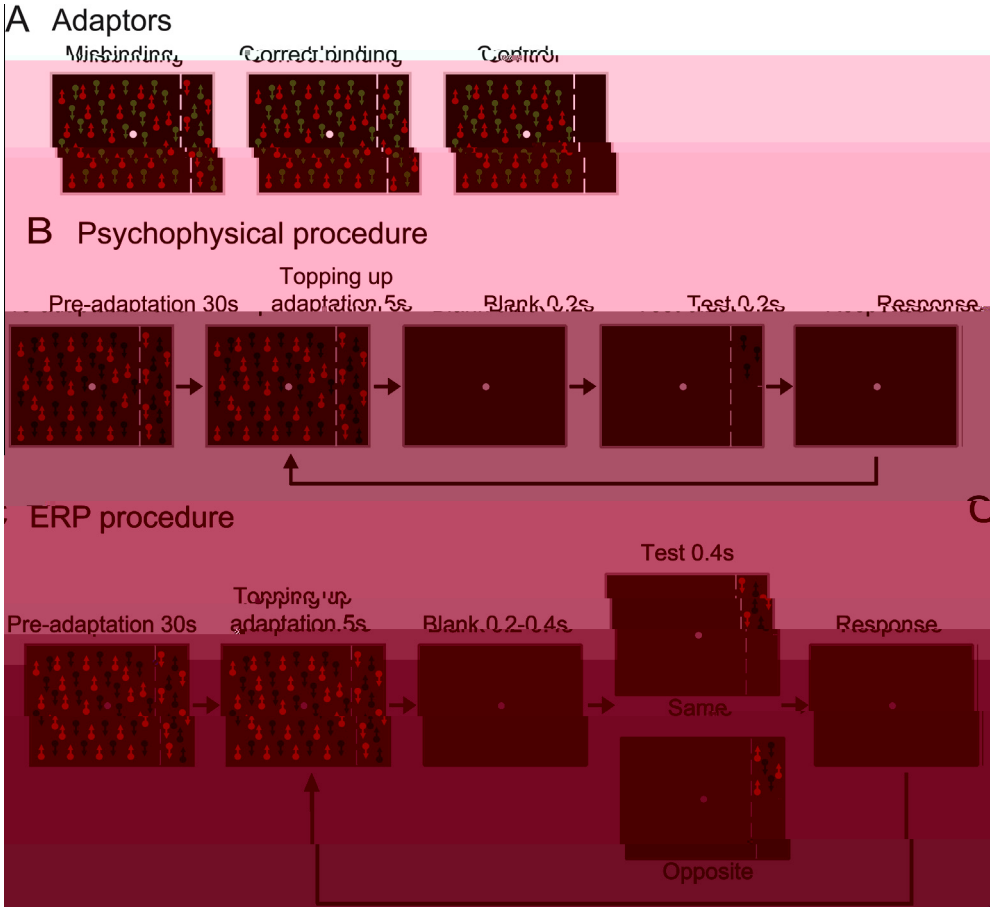

Fig. 1. Visual stimuli and experimental procedures. (A) Adaptors in the misbinding, correct binding, and control conditions. In the misbinding and correct binding conditions, adaptors contain both the induction part and the effect part, which are on the left and the right of the white dashed line, respectively. The dashed line is for illustration purposes only, which was not shown in the experiments. Adaptors in the control condition contain the induction part only. (B) Procedure of the psychophysical experiment. (C) Procedure of the ERP experiment. The same and opposite trials are illustrated here.

two adaptors, dots in the right end area (5.9 × 26.8 , effect part) and those in the rest area (23.6 × 26.8 , induction part) were rendered with different colors, either red (CIE (1931): x = 0.614, y = 0.344) or green (CIE (1931): x = 0.289, y = 0.593). For one adaptor, dots in the effect and induction parts of the upward-moving sheet were red and green, respectively. Dots in the corresponding parts of the downward-moving sheet were green and red, respectively. For the other adaptor, dots in the effect and induction parts of the upward-moving sheet were green and red, respectively. Dots in the corresponding parts of the downward-moving sheet were red and green, respectively. These two adaptors could induce the color-motion misbinding in the effect part. In the correct binding condition (Fig. 1A, the middle panel), the adaptors were identical to those in the misbinding condition except that, on both sheets of the adaptors, dots in the effect part and those in the induction part had the same color. The correct binding condition was included here for identifying neural processes associated with co-occurrence of color and motion. In the control condition (Fig. 1A, the right panel), the two adaptors contained the induction part only. The adaptors were counterbalanced in terms of color-motion pairing. The control condition was used as a baseline for measuring the CCMAEs in the misbinding and the correct binding conditions.

In the psychophysical experiment, there were 10 test stimuli. They were red or green dots presented in the upper half of the effect part area, with one of Þve different speeds (0.6 /s upward, 0.3 /s upward, 0 /s, 0.3 /s downward, 0.6 /s downward). In the ERP experiment, for each adaptor, there were two test stimuli, each of which contained both red and green dots moving in opposite directions. The dots in a test stimulus moved in the same or opposite direction to those in the effect part of the adaptor. Throughout the experiments, a white dot was presented at the display center and subjects needed to Þxate on it.

2.4. Psychophysical experiment

Using a method of constant stimuli, the psychophysical experiment was designed to measure the CCMAE in the three adaptation conditions. The experiment consisted of 60 blocks of 40 trials, 10 blocks for each adaptor. Each block started with a 30-sec pre-adaptation (Fig. 1B). On a trial, a test stimulus was presented for 0.2 s after a 5 s topping-up adaptation and a 0.2 s blank interval, and subjects made a 2-AFC judgment on the motion direction of the test stimulus (upward or downward). For each adaptor, each of the ten test stimuli was presented on 40 trials. The order of the three adaptation conditions/blocks was randomized across subjects.

2.5. Psychophysical data analysis

We Þrst constructed a psychometric function for each adaptation condition shown in Fig. 2A. We plotted the percentage of trials on which the test stimulus direction was perceived to be opposite to the physical direction of adapting dots (with the same color as

the test) as a function of the test speed. For each condition, the psychometric values at the Þve test speeds were Þt with a cumulative normal function. We interpolated the data to Þnd the speed expected to be perceived as stationary. The speed difference between the misbinding condition and the control condition was the CCMAE from adaptation to the color-motion misbinding in the effect part, and the speed difference between the correct binding condition and the control condition was the CCMAE from adaptation to the correct color-motion binding.

2.6. ERP experiment

The ERP experiment aimed to measure the color-contingent motion adaptation effect in the brain. It consisted of 36 blocks of 36 trials, 6 blocks for each adaptor. Similar to the psychophysical experiment, each block started with a 30 s pre-adaptation (Fig. 1C). On a trial, after a 5-sec topping-up adaptation and a 0.2Ð0.4 s blank interval, a test stimulus was presented for 0.4 s. Subjects needed to make a 2-AFC judgment on a near-threshold luminance change (increment or decrement) of the test stimulus for attentional control. The luminance change occurred between 0.2 and 0.4 s after the onset of the test stimulus. It was determined by QUEST staircases (Watson & Pelli, 1983) before the experiment to ensure that subjects performed equally well for all the adapting and test stimuli (75% correct). For each adaptor, each of the two test stimuli was presented on 108 trials. The order of the three adaptation conditions/blocks was randomized across subjects.

2.7. EEG recording

EEG was recorded from 64 scalp sites using Ag/AgCl electrodes mounted in an elastic cap (Brain Products, Munich, Germany) according to the extended international 10Ð20 EEG system. We recorded VEOG (vertical electro-oculogram) from an electrode positioned above the right eye and HEOG (horizontal electro-oculogram) from an electrode at the outer canthus of the left eye. The signals from the 64 scalp electrodes were referenced online to an electrode on the tip of the nose and were re-referenced ofßine to the mean signal from the left and right mastoids. Impedance for all the electrodes was kept below 5 k X. EEG was ampliÞed with a gain of 500 K, band-pass Þltered from 0.05 to 100 Hz, and digitized at a sampling rate of 1000 Hz.

2.8. ERP data analysis

We used Brain Vision Analyzer (Brain Products, Munich, Germany) to analyze EEG signals induced by the test stimuli. EEG data were Þrst low-pass Þltered at 30 Hz and then epoched from 100 ms before stimulus onset to 250 ms after stimulus onset. EEG epochs were corrected for baseline over the 100 ms interval immediately before stimulus onset. Eye-blink artifacts were semi-automatically corrected using the method proposed by Gratton, Coles, and Donchin (1983) . Any epoch exceeding ±50 l V at any electrode was excluded from analysis. Remaining epochs were selectively averaged according to the types of the test stimuli in which the red and green dots moved in the same (i.e., the same trial) or opposite (i.e., the opposite trial) direction to those in the effect part of the adaptor.

The C1 response was apparent between 60 and 100 ms after stimulus onset. To select electrodes for C1 amplitude and latency analysis, for each adaptation condition, grand averaged ERPs were made by averaging across subjects and test stimuli. Left posterior electrodes, including P1, P3, P5, PO3, PO7, POZ, O1, and Oz, had the largest C1 amplitudes, in all the three adaptation conditions.

2.9. Source localization

Estimation of dipole sources was performed using the Brain Electrical Source Analysis (BESA) algorithm (BESA version 5.3). For the misbinding and correct binding conditions, dipole modeling was carried out based on the difference waveforms between the same and opposite trials. We Þrst used one dipole with free location and orientation to Þt the distribution of the difference waveform in the 68Ð110 ms interval for the misbinding condition and in the 57Ð79 ms interval for the correct binding condition, respectively. The four-shell ellipsoidal head model was used. The initial starting position of the dipole was randomly chosen and using different starting locations yielded a highly similar dipole conÞguration. Then, we localized a dipole within area V1 to best account for the distribution of the difference waveform in the 68Ð110 ms interval for the misbinding condition and a dipole within area V2 to best account for the distribution of the difference waveform in the 57Ð79 ms interval for the correct binding condition, respectively.

3. Results

3.1. Psychophysical results

In the psychophysical experiment, we measured the CCMAE from adapting to the correct binding or the misbinding of color and motion in the effect part. After pre-adaptation and topping-up adaptation, a test stimulus (i.e., red or green moving dots) was presented brießy, and subjects made a 2-AFC judgment on the motion direction of the test stimulus (upward or downward) (Fig. 1B).

Because data from the red and green test stimuli showed a similar pattern, they were pooled together for analysis. Fig. 2A shows the psychometric functions in the three adaptation conditions. In the control condition, subjects adapted to the induction part only. Their performance was almost perfect for all the test stimuli (about 50% level for the 0 /s stimulus, good judgment for the 0.3 /s and 0.6 /s stimuli), demonstrating that adaptation to the induction part only generated little CCMAE in the effect part area. However, after adapting to the correct binding of color and motion, the psychometric function showed a leftward shift. This result demonstrated that subjectsÕ perception of the moving direction of the tests was biased opposite to the physical direction of the adapting dots (with the same color as the test). Strikingly, after adapting to the misbinding of color and motion, the psychometric function exhibited a rightward shift, showing that subjectsÕ perception of the direction of the tests was biased opposite to the perceived (rather than the physical) direction of the adapting dots. These results demonstrated that adaptation to the color-motion misbinding could generate the CCMAE and the CCMAEs in the misbinding and the correct binding conditions had opposite directions, suggesting that neurons in visual cortex might represent the color-motion misbinding for the dots in the effect part.

To quantitatively measure the CCMAE magnitude in each adaptation condition, psychometric values at the Þve test speeds were Þt with a cumulative gaussian function. We interpolated the data to Þnd the speed expected to be perceived stationary. We used the speed in the control condition as a baseline. The speed differences between the control condition and the correct binding condition (mean ± SEM: 0.17 ± 0.01 /s) and between the control condition and the misbinding condition (mean ± SEM: 0.13 ± 0.01 /s) were deÞned as the CCMAE magnitudes in the correct binding condition and the misbinding condition, respectively (Fig. 2B). Both the CCMAE magnitudes were signiÞcantly

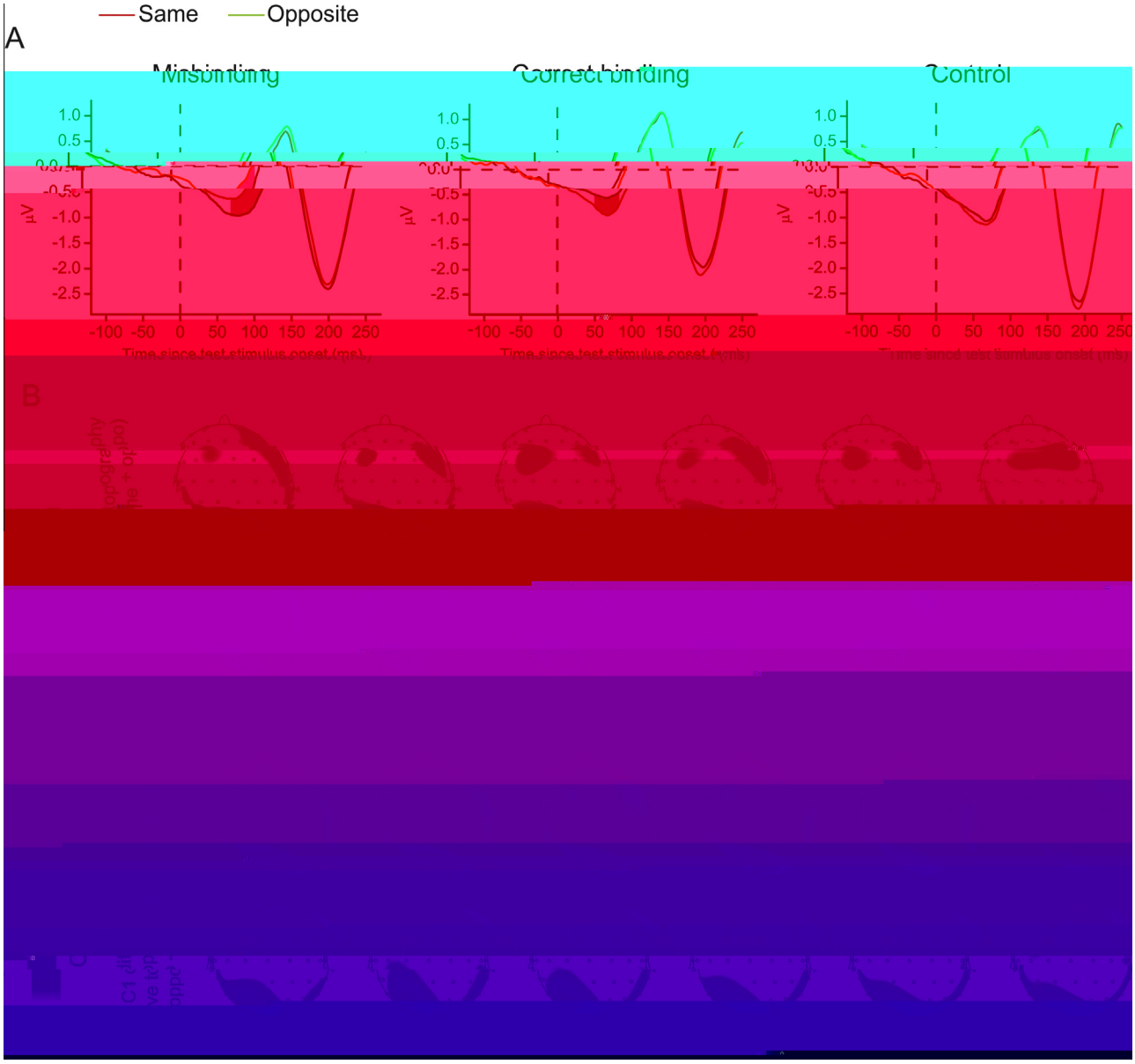

Fig. 3. ERP results. (A) ERPs averaged over the eight left posterior electrodes and all subjects in response to the test stimuli in the misbinding, correct bin ding, and control conditions. (B, C) Progression of the scalp voltage topography from 51 to 110 ms after stimulus onset in the misbinding and correct binding conditions . ÔÔsame + oppoÓ refers to the averaged topography between the same and opposite trials. ÔÔsame − oppoÓ and ÔÔoppoSameÓ refer to the difference topography between the same and opposite trials.

(68Ð110 ms after stimulus onset). However, for the correct binding condition, the C1 peak phase (57Ð79 ms after stimulus onset) exhibited signiÞcant difference. No signiÞcant difference was found in the control condition.

3.3. Dipole modeling of intracranial source

We carried out dipole modeling of intracranial sources of the C1 component with the BESA algorithm, based on the difference waveforms between the same and opposite trials. We searched for one dipole with free location and orientation that could best explain the distribution of the difference waveform over the 68Ð110 ms interval for the misbinding condition and over the 57Ð79 ms interval for the correct binding condition, respectively. In the misbinding condition (Fig. 4A), a dipole located in V2 (Talairach coordinates: −7, −90, −14, BrodmannÕs area 18) was identiÞed. It could account for 91.1% of the variance in the C1 scalp voltage distribution. A dipole within V1 (Talairach coordinates: −13, −95, −7, BrodmannÕs area 17) could best account for 78.9% of the variance. In the correct binding condition (Fig. 4B), a dipole located in V1 (Talairach coordinates: −11, −92, −7, BrodmannÕs area 17) was identiÞed. It could account for 89.8% of the variance. A dipole within V2 (Talairach coordinates: −4, −88, −15, BrodmannÕs area 18) could best account for 81.6% of the variance. We also performed an additional dipole localization analysis that was restricted to the time frames of the C1 peaks (i.e., the 7 data points around the C1 peak). The analysis generated a similar result.

3.4. Correlation analysis between psychophysical and ERP measures

To further evaluate the role of the C1 adaptation effects in the misbinding and correct binding of color and motion, we calculated the correlation coefÞcients between the CCMAE and the C1 adaptation index across 22 subjects who participated in both the

psychophysical and ERP experiments. The CCMAE was signiÞcantly correlated with the C1 adaptation index in both the misbinding ($r = 0.451$, $p = 0.035$) and correct binding ($r = -0.478$, $p = 0.024$) conditions (Fig. 5). Note that, according to the deÞnition of the C1 adaptation index (see the method part), in the misbinding condition, the stronger the adaptation effect, the most positive the index, resulting a positive correlation coefÞcient. However, in the correct binding condition, the stronger the adaptation effect, the more negative the index, resulting a negative correlation coefÞcient.

4. Discussion

Using psychophysical and ERP adaptation techniques, our study provides the following Þndings on the mechanisms of the color-motion misbinding. (1) Adaptation to the color-motion misbinding could generate a CCMAE. The direction of the CCMAE followed the prediction by the misbinding, opposite to the CCMAE direction from adaptation to the correct binding. This Þnding replicated our previous work (Zhang et al., 2014). (2) The peak latency of the C1 components induced by the test stimuli after adapting to the misbinding was about 11 ms later than that after adapting to the correct binding. (3) The reduced C1 amplitude (i.e., the C1

Electrophysiological studies in monkey subjects have found that color and motion are processed in different, yet mutually connected cortical pathways (Fellaman & Van Essen, 1991). It is widely accepted that the color processing pathway consists of the blobs of V1, the thin stripes of V2, and V4, and the motion processing pathway includes the layer 4B of V1, the thick stripes of V2, and V5/MT + (Bartels & Zeki, 2000; Sincich & Horton, 2005). Meanwhile, neurons selective for both color and motion direction were found in V1 (Gegenfurtner et al., 1996). Recently, using fMRI, Seymour, Clifford, Logothetis, and Bartels (2009) applied multivariate pattern analysis (MVPA) to decode subjectsÕ perception when they viewed color-motion conjunctions. It was shown that the physical feature conjunctions could be decoded from fMRI spatial activation patterns in early visual cortical areas, as early as in V1. This Þnding demonstrated an explicit representation of feature conjunctions at early visual processing stages, consistent with our Þnding in the correct binding condition. It is very likely that prolonged viewing of the correct binding of color and motion had adapted the dually selective neurons for color and motion direction in V1. This is why we found the C1 adaptation effect in the peak phase of the C1 component. Our Þnding here and Seymour et al.Õs Þnding might imply an early mechanism of visual feature conjunction. However, these Þndings cannot inform us whether the conjunction representation in early visual areas is the sensory coding of a feature pairing or the perceptual readout of a binding operation. We still do not know whether an active feature binding mechanism is indeed recruited for these unambiguous visual stimuli in these studies. Thus, to reveal the binding mechanisms, it is necessary to use visual stimuli that can induce feature misbinding.

Dually selective neurons for color and motion direction were much more common in V2 than V1 (Tamura, Sato, Katsuyama, Hata, & Tsumoto, 1996). Furthermore, Shipp, Adams, Moutoussis, and Zeki (2009) reported that such neurons are found more frequently in the superÞcial and deep layers (1, 2, 5, and 6) that receive feedback modulations from V4 and V5, relative to the intermediate layers (3 and 4) that relay ascending feedforward signals. We recently found that, after viewing the color-motion misbinding, the fMRI adaptation effect in V2 was closely associated with the CCMAE (Zhang et al., 2014). Furthermore, effective connectivity analyses showed that enhanced cortical feedback from V4 to V2 and from V5 to V2 might contribute to the misbinding. Our results in the misbinding condition are in line with these neurophysiological, anatomical, and fMRI Þndings. First, the peak latency of the C1 components in the misbinding condition was about 11 ms later than that in the correct binding condition. Second, the C1 adaptation effect in the misbinding condition was found in the descending phase of the C1 component, and the cortical source of the adaptation effect was identiÞed in V2. These two Þndings may reßect the later activation of neurons in the feedback layers of V2 by the test stimuli in the misbinding condition, relative to the neuronal activation in V1 by the test stimuli in the correct binding condition (Girard, Hupe, & Bullier, 2001).

In sum, the current study provides human electrophysiological evidence that active feature binding takes place in early visual cortex, but at later processing stages than feature co-occurrence. It complements and corroborates our previous fMRI Þndings. In the future, other misbinding and active binding phenomena can be probed to fully understand how the binding problem is solved, which is a key component of visual information processing.

Acknowledgments

This work was supported by NSFC 31230029, MOST 2015CB351800 and NSFC 31421003.

References

Ales, J. M., Yates, J. L., & Norcia, A. M. (2010). V1 is not uniquely identiÞed by polarity reversals of responses to upper and lower visual Þeld stimuli. NeuroImage, 52 (4), 1401Ð1409 .
Bartels, A., & Zeki, S. (2000). The architecture of the colour centre in the human visual brain: New results and a review. European Journal of Neuroscience, 12 172Ð193.
Blaser, T., Papathomas, Z., & Vidny‡nszky, Z. (2005). Binding of motion and colour is early and automatic. European Journal of Neuroscience, 2,12040Ð2044.
Bodel—n, C., Fallah, M., & Reynolds, J. H. (2007). Temporal resolution for the perception of features and conjunctions. Journal of Neuroscience, 27(4), 725Ð730.
Bouvier, S., & Treisman, A. (2010). Visual feature binding requires reentry. Psychological Science, 2,1200Ð204.
Chen, J., He, Y., Zhu, Z., Zhou, T., Peng, Y., Zhang, X., et al. (2014). Attention-dependent early cortical suppression contributes to crowding. Journal of Neuroscience, 34(32), 10465Ð10474 .
Clark, V. P., & Hillyard, S. A. (1996). Spatial selective attention affects early extrastriate but not striate components of the visual evoked potential. Journal of Cognitive Neuroscience, 8 387Ð402.
Colby, C. L., & Goldberg, M. E. (1999). Space and attention in parietal cortex. Annual Review of Neuroscience, 22(1), 319Ð349 .
Di Lollo, V. (2012). The feature-binding problem is an ill-posed problem. Trends in Cognitive Sciences, 16317Ð321.
Esterman, M., Verstynen, T., & Robertson, L. C. (2007). Attenuating illusory binding with TMS of the right parietal cortex. NeuroImage, 35(3), 1247Ð1255 .
Fellaman, D. J., & Van Essen, D. C. (1991). Distributed hierarchical processing in the primate visual cortex. Cerebral Cortex, 1 1Ð47.
Foxe, J. J., & Simpson, G. V. (2002). Flow of activation from V1 to frontal cortex in humans: A framework for deÞning ÔÔearlyÓ visual processing.Experimental Brain Research, 142 39Ð150.
Friedman-Hill, S. R., Robertson, L. C., & Treisman, A. (1995). Parietal contributions to visual feature binding: Evidence from a patient with bilateral lesions. Science, 269(5225), 853Ð855 .
Gegenfurtner, K. R., Kiper, D. C., & Fenstemaker, S. B. (1996). Processing of color, form, and motion in macaque are V2. Visual Neuroscience, 13 161Ð172.
Gibson, J. J., & Radner, M. (1937). Adaptation, after-effect and contrast in the perception of tilted lines. Journal of Experimental Psychology, 20 453Ð467.
Girard, P., Hupe, J. M., & Bullier, J. (2001). Feedforward and feedback connections between areas V1 and V2 of the monkey have similar rapid conduction velocities. Journal of Neurophysiology, 85(3), 1328Ð1331 .
Gratton, G., Coles, M. G., & Donchin, E. (1983). A new method for off-line removal of ocular artifact. Electroencephalography and Clinical Neurophysiology, 55(4), 468Ð484.
Guthrie, D., & Buchwald, J. S. (1991). SigniÞcance testing of difference potentials. Psychophysiology, 28 240Ð244.
Hoffmann, M. B., Unsšld, A. S., & Bach, M. D. (2001). Directional tuning of human motion adaptation as reßected by the motion VEP. Vision Research, 41(17), 2187Ð2194 .
Holcombe, A. O., & Cavanagh, P. (2001). Early binding of feature pairs for visual perception. Nature Neuroscience, 4 127Ð128.
Humphrey, G. K., & Goodale, M. A. (1998). Probing unconscious visual processing with the McCollough effect. Consciousness and Cognition, ,7494Ð519.
Jeffreys, D. A., & Axford, J. G. (1972). Source locations of pattern-speciÞc components of human visual evoked potentials. I. Component of striate cortical origin. Experimental Brain Research, 16 1Ð21.
Koivisto, M., & Silvanto, J. (2011). Relationship between visual binding, reentry and awareness. Consciousness and Cognition, 20(4), 1293Ð1303 .
Koivisto, M., & Silvanto, J. (2012). Visual feature binding: The critical time windows of V1/V2 and parietal activity. NeuroImage, 59 1608Ð1614.
Livingstone, M., & Hubel, D. (1988). Segregation of form, color, movement & depth: Anatomy, physiology and perception. Science, 240 740Ð749.
Mayhew, J. W., & Anstis, S. M. (1972). Movement aftereffects contingent on color, intensity, and pattern. Perception & Psychophysics, 12(1), 77Ð85.
Murray, M. M., Wylie, G. R., Higgins, B. A., Javitt, D. C., Schroeder, C. E., & Foxe, J. J. (2002). The spatiotemporal dynamics of illusory contour processing: Combined high-density electrical mapping, source analysis, and functional magnetic resonance imaging. Journal of Neuroscience, 22(12), 5055Ð5073 .
Robertson, L. C. (2003). Binding, spatial attention and perceptual awareness. Nature Reviews Neuroscience, (2), 93Ð102.
Seymour, K., Clifford, C. W., Logothetis, N. K., & Bartels, A. (2009). The coding of color, motion, and their conjunction in the human visual cortex. Current Biology, 19(3), 177Ð183 .
Shafritz, K. M., Gore, J. C., & Marois, R. (2002). The role of the parietal cortex in visual feature binding. Proceedings of the National Academy of Sciences, 99(16), 10917Ð10922 .
Shipp, S., Adams, D. L., Moutoussis, K., & Zeki, S. (2009). Feature binding in the feedback layers of area V2. Cerebral Cortex, 19 2230Ð2239.
Sincich, L. C., & Horton, J. C. (2005). Input to V2 thin stripes arises from V1 cytochrome oxidase patches. Journal of Neuroscience, 25 10087Ð10093.
Stromeyer, C. F. (1972). Contour-contingent color aftereffects: Retinal area speciÞcity. The American Journal of Psychology,227Ð235.
Tamura, H., Sato, H., Katsuyama, N., Hata, Y., & Tsumoto, T. (1996). Less segregated processing of visual information in V2 than V1 of the monkey visual cortex. European Journal of Neuroscience, 8300Ð309.

Treisman, A. (1996). The binding problem. Current Opinion in Neurobiology, 6(2), 171Ð178.
Treisman, A., & Schmidt, H. (1982). Illusory conjunctions in the perception of objects. Cognitive Psychology, 14(1), 107Ð141.
Watson, A. B., & Pelli, D. G. (1983). QUEST: A Bayesian adaptive psychometric method. Perception & Psychophysics, 33(2), 113Ð120.
Whitney, D. (2009). Neuroscience: Toward unbinding the binding problem. Current Biology, 19, 251Ð253.
Wolfe, J. M., & Cave, K. R. (1999). The psychophysical evidence for a binding problem in human vision. Neuron, 24(11Ð17), 111Ð125.
Wu, D. A., Kanai, R., & Shimojo, S. (2004). Vision: Steady-state misbinding of colour and motion. Nature, 429, 262.
Zhang, X., Qiu, J., Zhang, Y., Han, S., & Fang, F. (2014). Misbinding of color and motion in human visual cortex. Current Biology, 24(12), 1354Ð1360.
Zhang, X., Zhaoping, L., Zhou, T., & Fang, F. (2012). Neural activities in V1 create a bottom-up saliency map. Neuron, 73(1), 183Ð192.